Description of the 1C precipitation feature database

Chuntao Liu

Department of Physical and Environmental sciences
Texas A&M University at Corpus Christi
Chuntao.liu@tamucc.edu
http://atmos.tamucc.edu/trmm/

Version 1

7. 2017

1. Algorithm

1.1 GPM Precipitation Feature

The Precipitation Feature (PF) database summarizes the properties of PFs and has proven to be a very useful tool in studying the various types of precipitation systems and their contribution to global rainfall in the tropics and subtropics from TRMM (e.g., Nesbitt et al. 2000; Cecil et al. 2005; Liu et al. 2008; Romatschke et al. 2010; Zhou et al. 2013; Rasmussen et al. 2014; Houze et al. 2015). Appling the same principle, an algorithm for defining PFs using the GPM core satellite observations has been developed at Texas A&M University at Corpus Christi. An overview of the algorithm is shown in right side of Figure 1.

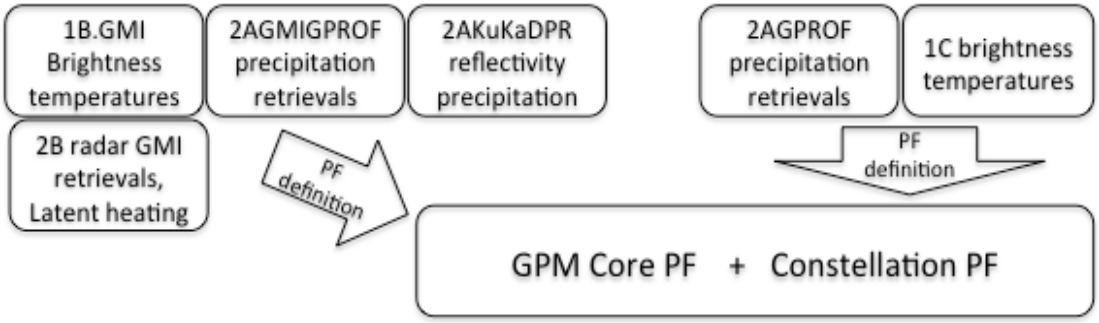

Figure 1. Workflow of the current GPM precipitation feature (PF) and constellation PF algorithm.

Currently the framework of the GPM PF algorithm includes a) combining useful parameters from each individual Ku, Ka, DPR and GMI products; b) collocating GMI high/low frequencies and Ku/Ka radar measurements after the parallax correction of the different geo-location geometry for nadir and conical scans; c) defining precipitation features; d) calculation of parameters representing the convective and precipitation properties inside the PF (
Table 1). This algorithm has been successfully implemented using new Version 4 GPM products. Since 2015, the GPM PFs have been used in the study of the global distribution of the most intense convection (Liu and Zipser 2015) and convection overshooting the tropopause (Liu and Liu 2016).

Table 1. Parameters calculated by the GPM PF algorithm for each PF.

	GPM PF Properties
Geo location	Location, time, size
Precipitation	Volumetric precipitation from Ku, Ka, DPR, GMI. Maximum precipitation rate
Intensity	Maximum 20, 30, 40 dBZ echo top heights; Minimum 37, 85 GHz PCT, 183 TB etc.
Vertical structure	Maximum reflectivity at 40 levels with 0.5 km interval, number of pixels with > 20, 30, 40 dBZ at 16 levels with 1 km interval
Morphology	Ellipse fit to the feature, center location, major, minor axis,

	orientation, solidity
Latent heating	Total, convective, and stratiform latent heating profiles from SLH (Shige et al. 2004, 2009) and CSH (Tao et al. 2006).

1.2 Constellation precipitation feature

After completing the GPM Core PF database, we have incorporate the GPM constellation passive microwave instruments listed in **Table 2** into the GPM PF workflow (**Figure 1**). Each instrument offers a different perspective of the microphysical properties of precipitation systems due to the variety of resolutions and channels. Therefore, a separate constellation PF has to be designed for each individual satellite/instrument. However, a common definition is still required to collectively interpret these PFs. We approach this by using surface precipitation rate estimates from the Goddard Profiling (GPROF) algorithm, which uses a Bayesian approach to retrieve consistent precipitation information from passive microwave measurements (Kummerow et al. 2015). This algorithm is applied by NASA's Precipitation Processing System (PPS) to the GPM inter-satellite calibrated brightness temperatures (i.e., level 1C products) to retrieve the global surface precipitation (i.e., 2AGPROF product; GPM GPROF ATDB 2014). This facilitates a common definition for the PFs in our workflow. For each PF, the size, center location, precipitation volume, and cold brightness temperature properties are calculated. From multiple satellites, the constellation PFs provide much large samples of the global precipitation systems and their properties to enhance our understanding of life cycles of precipitation and global water cycle.

Table 2. Satellites with passive microwave sensors that are currently part of the GPM constellation.

Satellite	Sensor	Swath (km)	Center Channel Frequency in GHz (Resolution in km)
GPM	GMI	850	10.65 (26), 18.7 (15), 23.8 (12), 36.5 (11), 89.0 (6), 165.5 (6), 183.31±[3,7] (6)
F16	SSMIS	1700	19.35 (45x74), 22.235 (45x74), 37.0 (28x45), 91.665 (13x16), 150 (13x16), 183.311±[1,3,7] (13x16)
F17			
F18			
GCOMW1	AMSR2	1450	6.925/7.3 (10), 10.65 (10), 18.7 (10), 23.8 (10), 36.5 (10), 89.0 (5)
METOPA	MHS	2180	89 (16), 157 (16), 183.311±[1, 3] (16), 190.31 (16)
METOPB			
NOAA18			
NOAA19			
SNPP	ATMS	2200	23.8 (75), 31.4 (75), 50.3 (32), 51.76 (32), 52.8 (32), 53.596±0.115 (32), 54.4 (32), 54.94 (32), 55.5 (32), 57.290344 (32), 88.2 (32), 165.5 (16), 183.31±[1, 1.8, 3, 4.5, 7] (16)

2. Data structure

The algorithm is developed with PYTHON language. It creates the PFs from each satellite orbit and saves into daily files. At TAMUCC, all the daily files are combined into monthly. All the combined monthly data are available at: http://atmos.tamucc.edu/trmm/data/gpm/1C_PF/

Common variables:

AREARAIN	Precipitation area (km^2)
AREARAIN_100MM	Area with precipitation rate > 100 mm/hr [km^2]
AREARAIN_10MM	Area with precipitation rate > 10 mm/hr [km^2]
AREARAIN_1MM	Area with precipitation rate > 1 mm/hr [km^2]
AREARAIN_20MM	Area with precipitation rate > 20 mm/hr [km^2]
AREARAIN_50MM	Area with precipitation rate > 50 mm/hr [km^2]
AREASNOW	Area with snow [km^2]
DAY	Day of month
ELEV	Elevation [m]
HOUR	UTC hour
LANDOCEAN	Flag for land (1) and ocean (0)
LAT	Geo-center Latitude [degree]
LON	Geo-center Longitude [degree]
MAXRAINRATE	Maximum precipitation rate [mm/hr]
MONTH	Month
ORBIT	Orbit number
R_LAT	Latitude center of fitted ellipse [degree]
R_LON	Longitude center of fitted ellipse [degree[
R_MAJOR	Major axis length of fitted ellipse [km]
R_MAJOR_DEGREE	Major axis length of fitted ellipse [degree]
R_MINOR	Minor axis length of fitted ellipse [km]
R_MINOR_DEGREE	Minor axis length of fitted ellipse [degree]
R_ORIENTATION	Orientation of fitted ellipse
R_SOLID	fraction of area filled in fitted ellipse [0-1]
VOLRAIN	Volumetric precipitation [mm/hr/km^2]
VOLRAIN_100MM	Volumetric precipitation from > 100mm/hr [mm/hr/km^2]
VOLRAIN_10MM	Volumetric precipitation from > 10mm/hr [mm/hr/km^2]
VOLRAIN_1MM	Volumetric precipitation from > 1mm/hr [mm/hr/km^2]
VOLRAIN_20MM	Volumetric precipitation from > 20mm/hr [mm/hr/km^2]
VOLRAIN_50MM	Volumetric precipitation from > 50mm/hr [mm/hr/km^2]
VOLSNOW	Volumetric precipitation from snow [mm/hr/km^2]
YEAR	Year

Special variables corresponding to each satellite channels:

AREA37LT175	Area with 37 GHz PCT < 175 K [km^2]
AREA37LT200	Area with 37 GHz PCT < 200 K [km^2]

AREA37LT225	Area with 37 GHz PCT < 225 K [km^2]
AREA37LT250	Area with 37 GHz PCT < 250 K [km^2]
AREA37LT275	Area with 37 GHz PCT < 275 K [km^2]
AREA89LT100	Area with 85 GHz PCT < 100 K [km^2]
AREA89LT125	Area with 85 GHz PCT < 125 K [km^2]
AREA89LT150	Area with 85 GHz PCT < 150 K [km^2]
AREA89LT175	Area with 85 GHz PCT < 175 K [km^2]
AREA89LT200	Area with 85 GHz PCT < 200 K [km^2]
AREA89LT225	Area with 85 GHz PCT < 225 K [km^2]
AREA89LT250	Area with 85 GHz PCT < 250 K [km^2]
AREA89LT275	Area with 85 GHz PCT < 275 K [km^2]
MINPCT37	Minimum 37 GHz PCT [K]
MINPCT89	Minimum 85 GHz PCT [K]

3. Reading software

Python:

```
def recursively_load_dict_contents_from_group(h5file, path):
    """This program reads in HDF5 file and load into a dictionary """
    ans = {}
    for key, item in h5file[path].items():
      if isinstance(item, h5py._hl.dataset.Dataset):
        ans[key] = item.value
      elif isinstance(item, h5py._hl.group.Group):
        ans[key] = recursively_load_dict_contents_from_group(h5file, path + key + '/')
    return ans
```

IDL:

http://atmos.tamucc.edu/trmm/data/software/hdf5_2_struct.pro

4. Addition of lightning data

First, an ellipse is fit to the PF area. Then the lightning strikes within the ellipse are identified to be associated to the PF. This methodology has several advantages comparing to the pixel level collocation—it includes lightning strikes that occurred a few minutes earlier or later, but near the storm area and largely addresses the motion and fast development/dissipation of the storms; b. it can be implemented starting from the precipitation feature level instead of one-one pixel collocation (pixel resolution varying between ISS-LIS and GLM) and can be calculated much more efficiently. An example is shown in Figure 2.

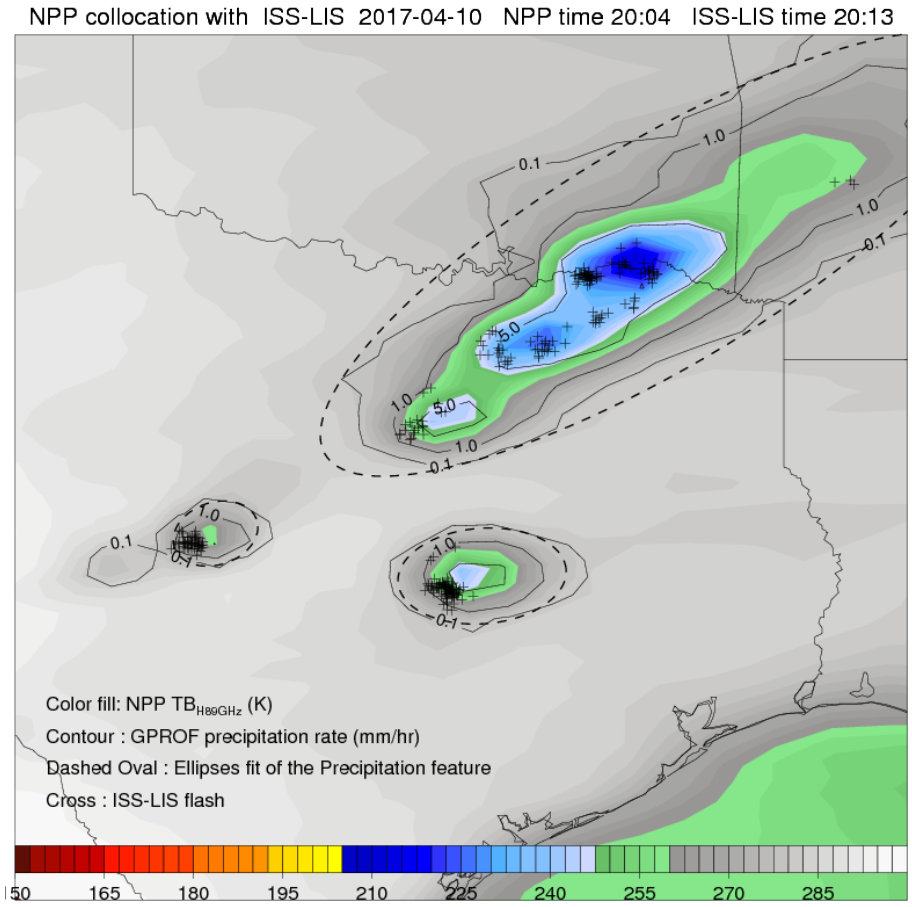

Figure 2. *An example of the collocation between 1C NPP satellite precipitation feature with the ISS-LIS lightning data. Color fill shows the 89 GHz PCT by NPP. Small crosses show the locations of ISS-LIS lighting.*

Currently (201707), additions of ISS-LIS and GOES-R lightning are planned, but not processed. Please contact us if you are interested in the dataset.

References

Cecil, D. J., S. J. Goodman, D. J. Boccippio, E. J. Zipser, and S. W. Nesbitt, 2005: Three Years of TRMM Precipitation Features. Part I: Radar, Radiometric, and Lightning Characteristics. *Mon. Weather Rev.*, **133**, 543–566, doi:10.1175/MWR-2876.1.

Houze, R. A., K. L. Rasmussen, M. D. Zuluaga, and S. R. Brodzik, 2015: The variable nature of convection in the tropics and subtropics: A legacy of 16 years of the Tropical Rainfall Measuring Mission satellite. *Rev. Geophys.*, **53**, 994–1021, doi:10.1002/2015RG000488.

Kummerow, C. D., D. L. Randel, M. Kulie, N.-Y. Wang, R. Ferraro, S. Joseph Munchak, and V. Petkovic, 2015: The Evolution of the Goddard Profiling Algorithm to a

Fully Parametric Scheme. *J. Atmos. Ocean. Technol.*, **32**, 2265–2280, doi:10.1175/JTECH-D-15-0039.1.

Liu, C., E. J. Zipser, D. J. Cecil, S. W. Nesbitt, and S. Sherwood, 2008: A Cloud and Precipitation Feature Database from Nine Years of TRMM Observations. *J. Appl. Meteorol. Climatol.*, **47**, 2712–2728, doi:10.1175/2008JAMC1890.1.

——, and E. J. Zipser, 2015: The global distribution of largest, deepest, and most intense precipitation systems. *Geophys. Res. Lett.*, **42**, 3591–3595, doi:10.1002/2015GL063776.

Liu, N., and C. Liu, 2016: Global distribution of deep convection reaching tropopause in 1 year GPM observations. *J. Geophys. Res. Atmos.*, **121**, 3824–3842, doi:10.1002/2015JD024430.

Nesbitt, S. W., E. J. Zipser, and D. J. Cecil, 2000: A Census of Precipitation Features in the Tropics Using TRMM: Radar, Ice Scattering, and Lightning Observations. *J. Clim.*, **13**, 4087–4106, doi:10.1175/1520-0442(2000)013<4087:ACOPFI>2.0.CO;2.

Rasmussen, K. L., M. D. Zuluaga, and R. A. Houze, 2014: Severe convection and lightning in subtropical South America. *Geophys. Res. Lett.*, **41**, 7359–7366, doi:10.1002/2014GL061767.

Romatschke, U., S. Medina, and R. A. Houze, 2010: Regional, seasonal, and diurnal variations of extreme convection in the South Asian region. *J. Clim.*, **23**, 419–439, doi:10.1175/2009JCLI3140.1.

Zhou, Y., W. K. M. Lau, and C. Liu, 2013: Rain characteristics and large-scale environments of precipitation objects with extreme rain volumes from TRMM observations. *J. Geophys. Res. Atmos.*, **118**, 9673–9689, doi:10.1002/jgrd.50776.